AGING STUDIES OF LOW pH CEMENT-BASED MATERIALS USED FOR ALUMINUM RADIOACTIVE WASTE CONDITIONING

T.A. LYCHAGINA[1*], D.I. NIKOLAYEV[1], M. BALASOIU[1,2], M. NICU[2], L. IONASCU[2], A.C. DRAGOLICI[2], F. DRAGOLICI[2]

[1] Frank Laboratory of Neutron Physics, Joint Institute for Nuclear Research, 141980 Dubna, Russia
**E-mail*: lychagina@nf.jinr.ru, *E-mail*: dmitry@nf.jinr.ru, *E-mail*: balas@jinr.ru
[2] "Horia Hulubei" National Institute of Physics and Nuclear Engineering, P.O.BOX MG-6, Bucharest-Magurele, Romania, *E-mail*: mnicu@nipne.ro, *E-mail*: laura_ionascu@nipne.ro, *E-mail*: adrag@nipne.ro, *E-mail*: fdrag@nipne.ro

Received June 29, 2018

Abstract. The microstructure of promising cement-based materials for the conditioning of low and intermediate level radioactive waste (LILW) was studied using neutron diffraction. In order to evaluate the stability of the hardened cement matrix and for taking into consideration the need for long-term durability in disposal conditions, the samples of cement-based materials were measured each year, in the period from 2016 to 2018, at the SKAT instrument in function at the IBR-2 reactor. The sample with the most stable composition was determined.

Key words: neutron diffraction, cement-based materials, radioactive waste, aging.

1. INTRODUCTION

Radioactive waste management is a very important issue nowadays and implies the conditioning of the waste in concrete as an embedding stable matrix. The matrix is the most important confinement barrier from radionuclide migration's point of view in the environment [1]. The cementitious materials developed for the encapsulation of radioactive waste must respect acceptance criteria, *i.e.* to have stable chemical, physical and mechanical properties for 300 years [2, 3]. Therefore, the monitoring during years of the structure of developed materials is a very important item.

To improve anticorrosive and mechanical properties of the conditioning matrices new methods and formulas are developed for several types of radioactive wastes subject either for long-term storage and/or for disposal [4-6]. For developing a suitable cement matrix to be used for metallic radioactive aluminum conditioning, the addition of inorganic [7] or organic [8, 9] components into the cement paste were investigated [10] in order to reduce the corrosion rate in alkaline solutions and to obtain a low permeability rate.

The internal structure of the cement-based materials can be studied with microscopy, X-rays and neutron scattering methods. The surface of a sample can be examined only by microscopy, while tens of microns of sample thickness can be investigated, using X-rays. The main advantage of the neutron method is that a depth of centimeters can be studied because of the high penetration capacity of the neutrons.

For example, pore distribution in two types (CEM V and CEM III) of cement-based materials was recently determined by neutron tomography [11]. The fundamental differences in the nature of neutron interactions with matter compared to X-rays provides additional benefits to neutron methods, including volumetric studies of massive objects [12], high sensitivity to water distribution [13] inside materials, and a notable visual contrast between light element-containing compounds.

Cementitious materials intended for radioactive waste encapsulation usually include substantial amounts of *Ordinary Portland Cement* (OPC) in their formulation.

Aluminum is a reactive amphoteric metal, readily forming a protective oxide layer on contact with air or water. This layer is generally regarded as stable in the pH range 4 ÷ 10. However, in a strongly alkaline medium, such as that encountered in conventional cementitious materials based on OPC, this layer is soluble, resulting in continued corrosion associated with liberation of hydrogen and subsequent formation of expansive metal hydroxides, in addition to calcium-based aluminosilicate hydrates. As a result, using Portland cement, or a composite cement (OPC blended with blast furnace slag and/or fly ash) to encapsulate wastes containing aluminum is prohibited.

Recent work [2, 6, 8] has shown that matrices obtained using CEM III-A and CEM V-A (which are commercially available) with addition of different ratio of $Al_2(SO_4)_3$, $C_6H_8O_7$, Pantarhol, $LiNO_3$ decrease the pH values and present very good mechanical characteristics, being the based for further investigations.

In the present paper preliminary results of neutron diffraction experiments on modified cementation system based on CEM III highlight aspects of aging processes, depending on the presence in samples of different admixed compounds.

The studies and results obtained are of high value being a basis for optimizing the cement matrix formulas and further developments, if necessary.

2. MATERIAL AND METHODS

2.1. SAMPLES DESCRIPTION

In the selection and evaluation process of suitable materials for radioactive metallic aluminum conditioning, a set of samples (presented in Table 1) was prepared based on a type of cement (CEM III) which demonstrate good mechanical behavior (see Table 1).

Table 1

The chemical compositions of studied cement samples

Sample composition
CEM III + H_2O + Al (powder)
CEM III + H_2O + Al (powder) + $Al_2(SO_4)_3$ + $C_6H_8O_7$ + pantarhol
CEM III + H_2O + Al (powder) + $Al_2(SO_4)_3$ + $C_6H_8O_7$ + pantarhol + $LiNO_3$

The structure of these samples is now under investigation by means of different neutron scattering and electron microscopy methods. The three-dimensional analysis performed by neutron tomography have shown that for cement-based samples, developed for the conditioning of aluminum radioactive waste, the admixture of specific additives leads to a substantial decrease in the number of pores produced by the introduction of aluminum powder [11]. In this way, it was confirmed by a direct method the improving quality of the cement matrix for the conditioning of aluminum by the addition of several chemical additives.

On the other hand, the samples prepared in March 2015 have been measured by means of neutron diffraction each year in the period from 2016 to 2018 to study the influence of aging on the structure changes.

2.2. NEUTRON DIFFRACTION MEASUREMENTS

The neutron diffraction experiments were performed at the neutron texture facility SKAT [14, 15] situated on the 7th beamline of the high flux pulsed nuclear reactor IBR-2 (FLNP, JINR, Dubna). The beam cross section is 50 by 90 mm. The entire cement sample was placed in the neutron beam and was involved in the formation of diffraction patterns (Figure 1).

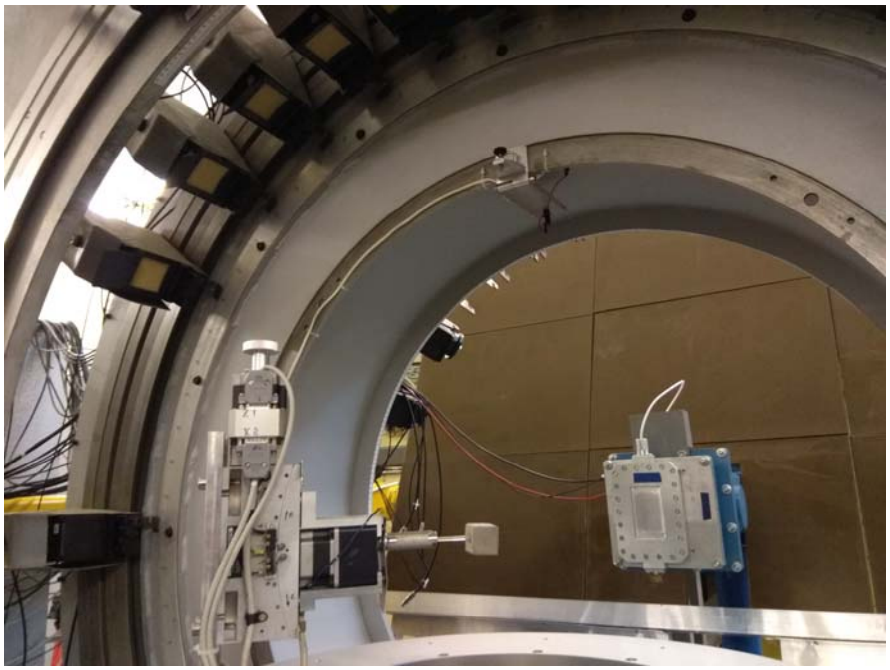

Fig. 1 – The image of SKAT diffractometer – the sample support inside the detector system.

In Figure 2 the scheme of the SKAT instrument is presented.

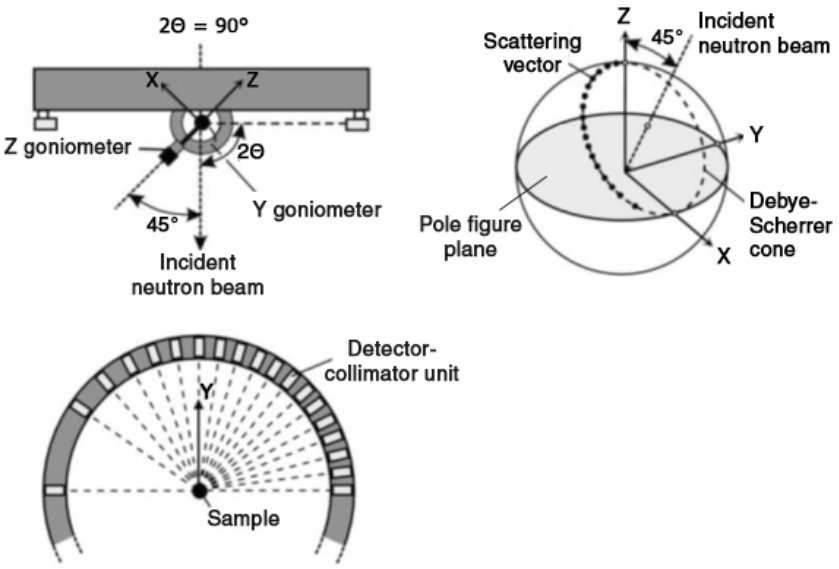

Fig. 2 – Scheme of the SKAT instrument.

The SKAT instrument is equipped with 19 He^3 detectors arranged at the same angle of 90º to the neutron beam. The system is also equipped with goniometers that allow the rotation of the sample around axis Z and Y (see Figure 1). Each detector at one sample position records a time-of-flight pattern. It can be seen from the figure that the detectors are not equally placed on the ring, but they are equally spaced on the line that is the intersection of the unit sphere and the Debye-Scherrer cone.

Diffraction patterns were measured on a grid of 5º to 5º in the reference coordinate system by rotating the specimen around the Z axis 360º in steps of 5º. Therefore, for each sample a number of $19 \times 72 = 1368$ individual patterns are recorded. By averaging all the diffraction individual patterns measured for 1368 spatial directions, the averaged information over the whole sample is obtained. The exposure time for one sample position was 1100 s, and for each hardened cement sample, the full measurements were continued for 22 hours. Each pattern contains 3100-time channels with counted neutrons for each channel. The relation between the neutron flight time and the neutron wavelength λ is the following:

$$t = \frac{L}{v} = \frac{m}{h} L\lambda,$$

where L is the total flight distance from the neutron source to the detector, v is the neutron velocity, m is the neutron mass, h is the Planck's constant. Thus, in a

detector situated at the angle 2ϑ with respect to the incident beam, the diffraction reflex will be in the time channel $t_{hkl} = \frac{m}{h} L d_{hkl} \sin(\vartheta)$, where $\lambda = d_{hkl} \sin(\vartheta)$ and d_{hkl} is the lattice spacing. In the case of the SKAT diffractometer for any detector $2\vartheta = 90^\circ$.

The SKAT diffractometer resolution, in the first approximation, can be expressed as follows

$$R = \frac{\Delta d}{d} = \sqrt{(\Delta t / t)^2 + (\Delta\vartheta / tg\vartheta)^2 + (\Delta L / L)^2}$$

The long flight (L = 103 m), as well as the presence of collimators in front of the detectors, provide a sufficiently high resolution $\Delta d / d = 5 \times 10^{-3}$ at $d = 2.5$ Å and $2\vartheta = 90^\circ$.

3. RESULTS

Before describing the results, we would like to emphasize that during the experiments the same samples were measured at exactly same conditions at the same instrument. Therefore, there is no influence on the results of any factors besides the internal changes within the samples themselves with the time.

The neutron diffraction patterns for the measured samples are shown in Figures 3-5. The large background values are connected with the water content in the samples. In other words, the large amount of water inside the hardened cement samples degrades the quality of the neutron diffraction pattern due to a large number of incoherent scattering effects. Nevertheless, the top of the patterns displays traces of the diffraction reflexes.

Despite the small signal/background ratio, the diffraction reflexes changes are statistically relevant because the diffraction patterns are obtained by summation of 1368 individual patterns measured for different orientations.

Figure 3 presents the diffraction pattern of the sample prepared on the base of *cement matrix with aluminum powder without any other additives*. Thus, this sample simulates the aluminum waste encapsulation in a cementitious matrix based on CEM III. As can be seen in Figure 3, two years after the first measurements (three years of aging) the almost all diffraction reflexes are grown up. This means that various processes inducing changes in the structure of the sample are still ongoing.

Figure 4 presents the diffraction pattern of the prepared sample on the modified CEM III-based system (with aluminum powder, $Al_2(SO_4)_3$, $C_6H_8O_7$ and Pantarhol). It can be seen from Figure 4 that this sample composition almost does not lead to structural changes after three years of aging.

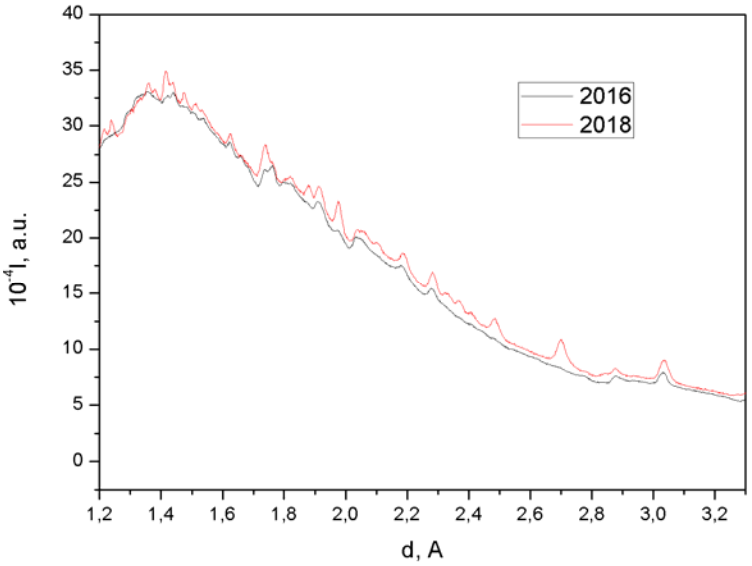

Fig. 3 – Neutron diffraction pattern for the sample composed of CEM III + H_2O + Al powder. The sample is prepared at March, 2015.

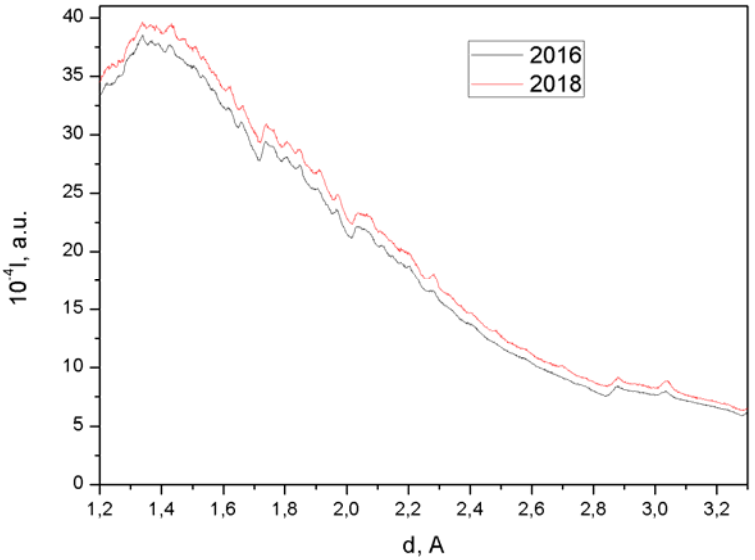

Fig. 4 – Neutron diffraction pattern for the sample composed of CEM III + H_2O + Al (powder) + $Al_2(SO_4)_3$ + $C_6H_8O_7$ + Pantarhol. The sample was prepared on March, 2015.

Figure 5 presents the diffraction pattern of the sample prepared on the modified system based on CEM III (with aluminum powder, $Al_2(SO_4)_3$, $C_6H_8O_7$, Pantarhol, and $LiNO_3$).

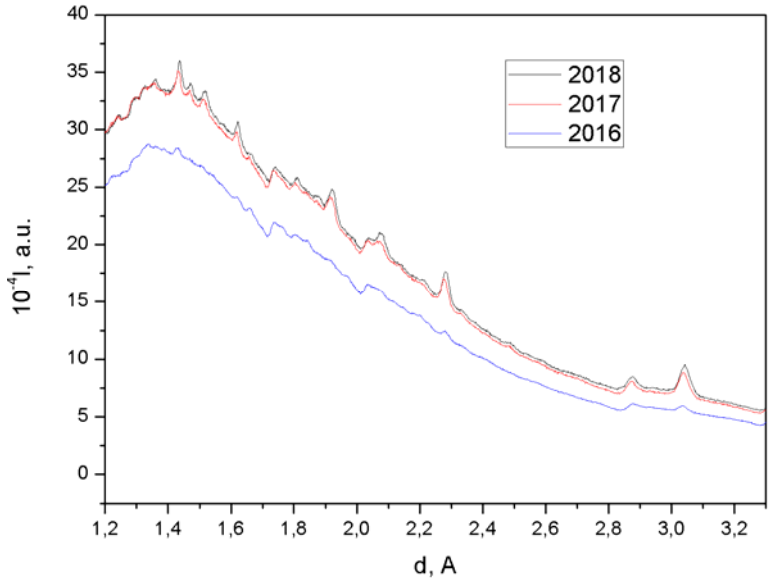

Fig. 5 – Neutron diffraction pattern for the sample composed of CEM III + H_2O + Al (powder) + $Al_2(SO_4)_3$ + $C_6H_8O_7$ + Pantarhol + $LiNO_3$. The sample is prepared at March, 2015.

It can be seen from the Figure 5 that this sample composition leads to changing structure processes after three years of aging. Moreover, the main changes took place in the period between the first and second measurements (after two years of aging). However, some diffraction reflexes keep growing after three years of aging.

Besides this effect, we observed the growth of the background in the neutron diffraction patterns between the first and second measurements (after two years of aging) (see Figure 5). Usually this phenomenon is associated with the amount of hydrogen increasing. In our case it could be interpreted as an hydrogen release due to the cement-aluminum reaction.

It is possible to interpret the diffraction reflexes existence as structural anisotropy presence in the hardened cement sample. This phenomenon can essentially influence the physical and the mechanical properties of cement-based materials and hence radioactive waste encapsulation.

Three years of aging samples showed that the process is not yet completed. To determine the stability of cement-based materials for the encapsulation of radioactive aluminum waste, we need to continue the annual study of the developed samples until the changes in the diffraction pattern become insignificant.

In the future, we intend to continue the investigations on other types of cement-based matrices and new sets of samples to look also specifically at the influence of the preparation technique.

4. CONCLUSIONS

Based on the presented results, we can summarize our conclusions as follows.

All the samples containing aluminum powder shows the growth of the diffraction reflexes in the neutron patterns except the sample containing $Al_2(SO_4)_3$, $C_6H_8O_7$ and Pantarhol.

It should be noted that in time the sample containing CEM III + H_2O + Al powder shows an increase in more phases than the sample with Al_2 $(SO_4)_3$ + $C_6H_8O_7$ + Pantarhol + $LiNO_3$, but the latter shows a more intensive growth of reflexes. Although the peak growth slows down after the first measurements, it does not completely stop.

We would like to emphasize once again the fact that reflexes growth means continuing structural changes process in the sample.

This can lead to anisotropy of the physical properties of the sample in time. We can say that from the point of view of structural stability is preferable to sample without $LiNO_3$.

Acknowledgments. This work was supported by the Joint Institute for Nuclear Research (04-4-1121-2015/2020; RO-JINR Projects Nos. 219/10.04.2017 and 220/10.04.2017 item 42, RO-JINR Projects Nos. 323/21.05.2018 item 61 and 322/21.05.2018 item 61).

REFERENCES

1. International Atomic Energy Agency, Characterization of Radioactive Waste Forms and Packages, Technical Report Series **383**, IAEA, Vienna, 1997.
2. F. Dragolici, M. Bucataru-Nicu, L. Lungu, C.N. Turcanu, Gh. Rotarescu, Durability of cemented waste in repository and under simulated conditions, IAEA-TECDOC-1397 137 (2004).
3. M. Nicu, L. Ionascu, C. Turcanu, F. Dragolici, Gh. Rotarescu, Gh. Dogaru, The influence of the complexing agents on the concrete matrix studied by XRD, Rom. Journ. Phys. **53**(7–8), 841–850 (2008).
4. J.R. Helliwell, J. Appl. Cryst. **47**, 4–5 (2014).
5. M. Najdoski, V. Koleva, S. Demiri, S. Stojkovikj, Mater. Res. Bull. **47**, 2239–2244 (2012).
6. A.I. Onuchukwu, Materials Chemistry and Physics **20**, 323 (1988).
7. M. Nicu, L. Ionascu, C. Turcanu, F. Dragolici, Rom. J. Phys. **60**, 1193–1202 (2015).
8. T. Matsuo, T. Nishi, M. Matsuda, Trans. Am. Nucl. Soc. **72**, 76 (1995).
9. M. Nicu, L. Ionascu, C. Turcanu, F. Dragolici, Gh. Rotarescu, Rom. J. Phys. **59**, 360–368 (2014).
10. L. Ionascu, M. Nicu, C. Turcanu, F. Dragolici, Gh. Rotarescu, Rom. Rep. Phys. **65**, 1512–1518 (2013).
11. S.E. Kichanov, K.M. Nazarov, D.P. Kozlenko, M. Balasoiu, M. Nicu, L. Ionascu, A.C. Dragolici, F. Dragolici, B.N. Savenko, Rom. J. Phys. **64**, 803 (2019).
12. I.S. Anderson, R. L. McGreevy, H. Z. Bilheux, *Neutron Imaging and Applications: A Reference for the Imaging Community*, Springer, New York, 2009.
13. H. Justnes, K. Bryhn-Ingebrigtsen, and G. O. Rosvold, Adv. Cem. Res. **6**(22), 67–72 (1994).
14. K. Ullemeyer, P. Spalthoff, J. Heinitz, N.N. Isakov, A.N. Nikitin, K. Weber, Nuclear instruments & methods in physics research, **412**(1), 80–88 (1998).
15. R. Keppler, K. Ullemeyer, J.H. Behrmann, M. Stipp, Journal of Applied Crystallography, 47, 1520–1535 (2014).